



Lattice Boltzmann 3D flow simulations on a metallic foam

Djomice Beugre^{a,*}, Sbastien Calvo^a, Grard Dethier^b, Michel Crine^a, Dominique Toye^a, Pierre Marchot^a

^a Department of Applied Chemistry, University of Lige, B-4000 Lige, Belgium

^b Department of Electrical Engineering and Computer Science, University of Lige, B-4000 Lige, Belgium

ARTICLE INFO

Article history:

Received 12 September 2008

Received in revised form 15 June 2009

Keywords:

Lattice Boltzmann method

X-ray micro-tomography

Metallic foam

Ergun's equation

ABSTRACT

In this paper a lattice Boltzmann method (LBM) is used to simulate isothermal incompressible flow in a RCM-NCX-1116 metallic foam. The computational technique is a multiple relaxation time (MRT) lattice Boltzmann equation model. Computer aided X-ray micro-tomography is used to obtain 3D images of the metallic foam, providing the geometry and information required for LB simulations of a single phase flow.

Pressure drops are computed and successfully compared to experimental measures and correlated with Ergun's equation. Invariance of Ergun's parameters A and B with the sampling rate of the images is observed.

© 2009 Elsevier B.V. All rights reserved.

1. Introduction

Recent progress in experimentation in macro- and micro-X-ray computed tomography allows visualization of complex geometries encountered in various fields of chemical engineering. In the domain of unit operations, high energy X-ray tomography (up to 420 kV) may be operated on rather large size equipments (e.g., columns of max. 0.5 m diameter and several meters height) with resolution down to a few tenths of mm. In the domain of materials, X-ray micro-tomographic devices are commonly available at 100 kV energy for samples of around 35 mm with resolutions close to 5 μm .

Consequently, it is natural to look forward to more accurate descriptions of phenomena occurring in packed beds, fibrous media, metallic foams, to name a few. This will lead to better design of elements, better efficiency and higher selectivity of chemical engineering processes in which they take place. Likely, the use of efficient computational fluid dynamic codes should help reaching these goals. However, the problem of incorporating these intricate geometries in simulation codes is challenging. Indeed, the numerical reconstructions, from these tomographic measurements lead to large matrices of voxels which must be used as boundaries for the flows. However, it is nearly impossible to realize surface meshing of these porous media geometries and consequently, to use classical CFD codes.

Lattice Boltzmann methods can easily accommodate directly these matrices but require large computing powers. Lattice Boltzmann (LB) are versatile methods extremely interesting to describe flows through highly complex geometries (porous media, packed beds, multiphase flows) [1,2], able to integrate multiphysics problems without any of the underlying semi-empirical homogenisation models, generally used in engineering applications.

In this paper, we consider the deployment of an in-house 3D lattice Boltzmann code on a computing grid to simulate a single phase flow within a metallic foam, a versatile material applied in many branches of engineering. We discuss briefly some results concerning the friction factor computed on the foam by simulations. X-ray tomographic devices used in this study are those available in the facilities of the **ULg** Chemical Engineering Laboratory [3].

* Corresponding address: Universite de Lige, Department of Applied Chemistry Laboratory of Chemical Engineering, Allee de la Chimie 3, Bat B6, 4000 Lige, Belgium.

E-mail address: da.beugre@ulg.ac.be (D. Beugre).

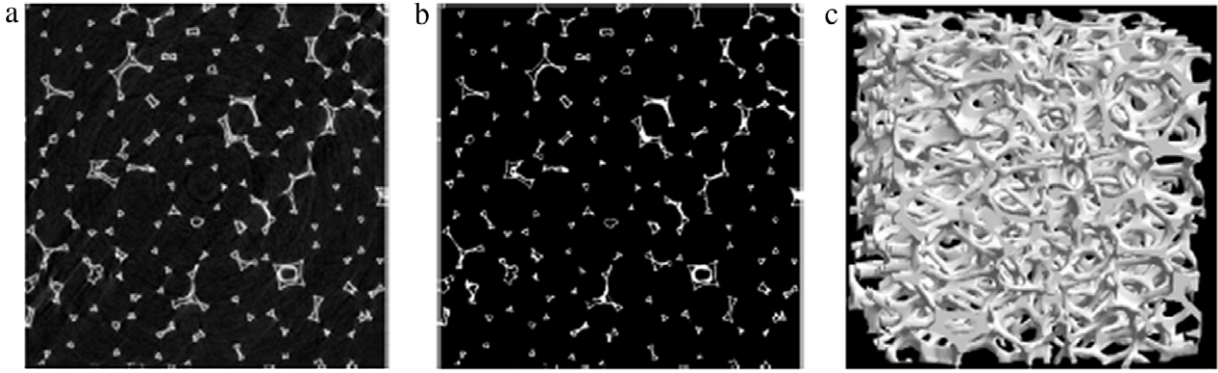


Fig. 1. The 2D and 3D structures of the metallic foam: (a) raw image, (b) thresholded and binarized image and (c) 3D reconstruction of the sample of size 12.8 mm^3 .

2. Metallic foam

The metallic foam (RCM-NCX-1116) is a Ni–Cr foam manufactured by Recemat International B.V. (The Netherlands). It has an extremely open cell structure which is obtained from a polyurethane foam, which is metallized. That metal coating is the framework of the metallic foam. The polyurethane is burnt away in a subsequent process. What remains are hollow struts of pure nickel. Generally these struts are more or less triangular. This hollow structure is then metallized with chromium in a further step. This adds an additional layer of metal on the structure and decreases the pore diameter. The micro-tomography of a sample of metallic foam ($12.8 \times 12.8 \times 12.8 \text{ mm}^3$) allows the reconstruction of 2D images of horizontal cross sections through the foam sample. Fig. 1a shows a 2D reconstructed section of the foam obtained by micro-tomography. This image contains 400×400 pixels, size of the pixel is equal to $32 \mu\text{m}$. The 2D sections are thresholded following the Otsu's method implemented in the MATLAB Image Processing Toolbox and then binarized. The internal porosity in the solid struts are not filled. Fig. 1b is the resulting thresholded and binarized image. Finally, the 3D structure is obtained by stacking these 2D sections, as illustrated in Fig. 1c. Using the large ULg 420 kV high energy tomograph operating in radiographic mode, we determine the characteristic pore diameter of the foam by computing the autocorrelation function of X-ray attenuations recorded on 200 lines of 1000 pixels of 0.37 mm width [4]. This leads to an average pore diameter of 2 mm and to a characteristic length of 62.5 pixels.

3. Lattice Boltzmann method

The lattice Boltzmann method (LBM) [5,6] is a recently developed numerical scheme that solves the microscopic lattice Boltzmann transport equation (LBE) rather than the Navier–Stokes (NS) equation. The Boltzmann equation is valid in principle over a wider range of flow physics than the NS equations. In LBM, microscopic fluid physics is simplified to retain only key elements (the local conservation laws and related symmetries) needed to guarantee accurate macroscopic behaviour.

Instead of solving the usual continuum hydrodynamic equations, e.g., NS equations, LBE deals with the evolution of discretized single-particle velocity distribution functions of fictitious particles. The ensuing lattice-based equation conserves mass, momentum, and energy. The local macroscopic quantities such as density and momentum are computed from the moments of these distribution functions [7]. Pressure is obtained from the state equation of isothermal ideal gas [8],

$$P = c_s^2 \rho. \quad (1)$$

Numerical implementation of LBE is simple and straightforward. In general, it consists of two computational substeps: relaxation (collision) and advection (streaming). We supply a brief introduction to the LBE scheme in the context of the D3Q19 lattice model. In this model, the 3D discrete phase space is defined by a cubic lattice with 19 discrete particle velocities $\{\mathbf{e}_\alpha \mid \alpha = 0, 1, \dots, 18\}$ as:

$$\mathbf{e}_\alpha = \begin{cases} (0, 0, 0) & \alpha = 0 \\ (\pm 1, 0, 0), (0, \pm 1, 0), (0, 0, \pm 1) & \alpha = 1, \dots, 6 \\ (\pm 1, \pm 1, 0), (\pm 1, 0, \pm 1), (0, \pm 1, \pm 1) & \alpha = 7, \dots, 18. \end{cases} \quad (2)$$

In a single relaxation time (SRT) lattice Boltzmann equation (LBE) model, the collision operator only involves a single relaxation time through Bhatnagar–Gross–Krook (BGK) approximation [9] so that all the moments of the distribution functions relax with the same time scale. This relaxation time τ is determined from the fluid viscosity ν . The ensuing collision operator is easy to implement, leading to widespread use of this model.

The SRT-LBE is given as:

$$f_\alpha(\mathbf{r} + \mathbf{e}_\alpha \delta_t, t + \delta_t) = f_\alpha(\mathbf{r}, t) - \frac{1}{\tau} [f_\alpha(\mathbf{r}, t) - f_\alpha^{(\text{eq})}(\mathbf{r}, t)], \quad (3)$$

where f_α and $f_\alpha^{(\text{eq})}$, $\alpha = 0, \dots, 18$, represent the 19 distribution functions and their equilibria, respectively; δ_t is the discrete time-step size.

The equilibria for incompressible flow are [10]

$$f_\alpha^{(\text{eq})} = w_\alpha \left\{ \delta\rho + \rho_0 \left[\frac{3\mathbf{e}_\alpha \cdot \mathbf{u}}{c^2} + \frac{9(\mathbf{e}_\alpha \cdot \mathbf{u})^2}{2c^4} - \frac{3u^2}{2c^2} \right] \right\} \quad (4)$$

where $\delta\rho$ is the density fluctuation, ρ_0 is the constant mean density of system, and $c = \delta_x/\delta_t$. In LBM the values of ρ_0 , δ_t and δ_x are typically set to unity. The sound speed in this model is $c_s = c/\sqrt{3}$. The total density is $\rho = \rho_0 + \delta\rho$. The weighting factors w_α for D3Q19 model are $w_0 = 0$, $w_{1,\dots,6} = 1/18$, $w_{7,\dots,18} = 1/36$, \mathbf{u} is the macroscopic velocity. The mass and momentum conservations are strictly enforced:

$$\delta\rho = \sum_\alpha f_\alpha = \sum_\alpha f_\alpha^{(\text{eq})}, \quad (5)$$

$$\rho_0 \mathbf{u} = \sum_\alpha \mathbf{e}_\alpha f_\alpha = \sum_\alpha \mathbf{e}_\alpha f_\alpha^{(\text{eq})}. \quad (6)$$

The Chapman–Enskog expansion [11] can be used to derive the fluid dynamic Navier–Stokes equation from the lattice Boltzmann equation (Eq. (3)).

The multiple relaxation time (MRT) lattice Boltzmann equation (LBE) model was developed by [12] at about the same time as the lattice BGK model. The MRT-LBE model has the same computational components, relaxation (collision) and advection (streaming), as the SRT-LBE model. The significant difference between these two models is in the collision operator. With the use of multiple relaxation times, MRT-LBE enables different moments to relax at different time rates.

In the formulation of the linear Boltzmann equation with multiple relaxation time approximation, the lattice Boltzmann evolution equation is written as [13]

$$f_\alpha(\mathbf{r} + \mathbf{e}_\alpha \delta_t, t + \delta_t) - f_\alpha(\mathbf{r}, t) = -M^{-1} \hat{S} [\mathbf{m}(\mathbf{r}, t) - \mathbf{m}^{(\text{eq})}(\mathbf{r}, t)]. \quad (7)$$

The bold-face symbol represents a column vector, e.g. $\mathbf{f} \equiv [f_0, f_1, \dots, f_{18}]^T$. Notations moments of \mathbf{m} and $\mathbf{m}^{(\text{eq})}$ are used to represent the 19 moments of \mathbf{f} and the corresponding equilibria of \mathbf{m} , respectively. The transformation matrix M will be described below. The diagonal collision matrix \hat{S} is defined as:

$$\hat{S} \equiv \text{diag}(1, s_1, s_2, 1, s_4, 1, s_4, 1, s_4, s_9, s_2, s_9, s_2, s_9, s_9, s_9, s_9, s_{16}, s_{16}, s_{16}) \quad (8)$$

the s_i , $i = 1, 2, 4, 9, 16$ are parameters corresponding to various relaxation time scales. In MRT-LBE, particle collision occurs in a moment space spanned by \mathbf{m} , while particle streaming happens in a velocity space spanned by \mathbf{f} . The spaces are related through a linear mapping: $\mathbf{m} = M\mathbf{f}$ or $\mathbf{f} = M^{-1}\mathbf{m}$. The transformations of $\mathbf{m}^{(\text{eq})}$ and the values of M and \hat{S} for D3Q19 lattice model can be found [14]. The kinetic viscosity ν and the bulk viscosity ς of this model are:

$$\nu = \frac{1}{3} \left(\frac{1}{s_9} - \frac{1}{2} \right) \quad \text{and} \quad \varsigma = \frac{2}{9} \left(\frac{1}{s_1} - \frac{1}{2} \right). \quad (9)$$

3.1. Analytical analysis for describing pressure drop characteristic of flow through foam metallic

Usually, the idea behind the analytical description of a viscous flow through porous media is to obtain a relation describing the pressure drop (∂xP) as a function of the porous media geometry (e.g., porosity, specific surface), the fluid properties (density, viscosity) and flow parameters (velocity),

$$\partial xP = f(\text{geometry}, \text{fluid}, \text{flow}). \quad (10)$$

In the literature, numerous authors (see, e.g., [15,16]) report on the use of Ergun's equation to estimate the pressure drop in porous media and for the calculation of friction factor.

The friction factor in a porous media is generally defined as;

$$f_k = \frac{\Delta P}{L} \frac{D_p}{\rho u^2} \frac{\varepsilon^3}{1 - \varepsilon} \quad (11)$$

and correlated as a function of the Reynolds number:

$$f_k = A \frac{1 - \varepsilon}{Re} + B \quad (12)$$

where ε is the porosity of the porous media (in the study $\varepsilon = 0.955$) and $Re = uD_p/\nu$ is the Reynolds number. u is the superficial velocity of the fluid, ρ the density and ν the kinematic viscosity. A and B are two constants related to the porous media medium. The characteristic length in this equation is the equivalent particle diameter (D_p) of the porous media defined by $D_p = 6/S_V$, where S_V is the surface area per unit volume of solid phase.

The equivalent particle diameter D_p is determined from the value of mean pore diameter d which is obtained by the method described above (cf. Section 2). d is defined by:

$$d = \frac{4\varepsilon}{S_V(1-\varepsilon)}. \quad (13)$$

The relationship of the mean pore diameter d and of the particle diameter D_p is thus given by:

$$D_p = \frac{3(1-\varepsilon)}{2\varepsilon}d. \quad (14)$$

Based on the empirical model of Ergun, the pressure drop (in a porous media) is generally computed as:

$$\frac{\Delta P}{L} = \frac{\rho}{D_p} \frac{(1-\varepsilon)}{\varepsilon^3} \left[A \frac{(1-\varepsilon)}{Re} + B \right] u^2. \quad (15)$$

3.2. Lattice unit conversion

One of the key components for the application of the lattice Boltzmann method to physical world problems is the correct conversion from lattice units to physical world units. In order to do so, we supply for fundamental quantities: length, time and mass, three conversion factors Δx , Δt , Δm by which we multiply quantities of the LB world to obtain corresponding physical world quantities.

$$l_{LB} \Delta x = L, \quad t_{LB} \Delta t = T, \quad m_{LB} \Delta m = m. \quad (16)$$

l_{LB} is the number of lattice nodes in the characteristic direction, L , is the physical characteristic length, ρ_{LB}^{ref} is the reference density in the LB world and ρ_{phys}^{ref} is the fluid physical density. The conversion factors may be determined as follows:

$$\Delta x = \frac{L}{l_{LB}}, \quad \Delta t = \Delta x \frac{c_s}{a}, \quad \Delta m = (\Delta x)^3 \frac{\rho_{phys}^{ref}}{\rho_{LB}^{ref}}, \quad (17)$$

where a , is the physical speed of sound. Now, we can obtain all other quantities by multiplying the unitless lattice Boltzmann quantities by the corresponding factors to obtain physical world values.

Although $P_{phys} = [\Delta m / (\Delta x (\Delta t)^2)] P_{LB}$, replacing Δm by its expression Eq. (17), the conversion factor of the mass is not needed to obtain Ergun's equation in the physical world.

4. Computational grid

Lattice Boltzmann methods need a lot of computational and memory resources. They either need very powerful machines or computational grids. The latter solution has the advantage of being economically more interesting. The grid software (LaBoGrid) we developed [17] does automatic work distribution among the machines of the grid. It associates one (or more) sub-lattice(s), representing parts of the discretized space, (cf. Section 3), to each CPU. A sub-lattice is a parallelepiped partition of the initial lattice. In the ideal case, each machine will receive as many sub-lattices as it has CPUs. The CPUs discovery is done by deploying an agent on each machine of the grid. This agent contacts the grid controller and sends him the detected number of CPUs. When all the agents have registered themselves to the controller, it creates the lattice partition and sends their parameters to each agent. The agents will then create a thread for each received sub-lattice. All communications are done using the message passing paradigm. The grid may be heterogeneous (various CPU types), the software takes into account the speed of the various CPUs and is fault tolerant. At the present state of development, the controller which needs only to possess a large memory is an AMD opteron dual core 256 2 GHz whereas the grid members are the four cores of a Xeon 5630, 2 GHz. On a $(200)^3$ lattice, 1000 iterations take 8 h, convergence may necessitate 10.000 iterations. A multiple relaxation time lattice Boltzmann algorithm (MRTLb) is used to simulate the flows through the metallic foam. The lattice chosen is a D3Q19 assuming periodic boundary conditions on faces parallel to the flow direction. A pressure gradient is applied between the entrance and exit faces. On the solid, full way bounce back conditions are used [18]. The equilibrium distribution corresponds to an incompressible fluid.

5. Numerical results and discussions

We simulated the flow through the metallic foam, considering different spatial scales in order to verify that A and B are actually independent of these scales which are obtained by undersampling homogeneously the initial 3D voxels matrix. We checked that this procedure kept the porosity constant within 1% (absolute). Flow simulations are performed using the MRT-LBE code of the LaBoGrid. The boundary conditions are the same as above (cf. Section 2). Among the 19 relaxation times, 5 are fixed by the selected viscosity, the others are those of [14].

Fig. 2a and b illustrate the distribution of the velocity component parallel to the flow direction in planes perpendicular and parallel to the flow direction, respectively, with a undersampling (200^3 voxels) of the initial 3D voxels matrix. Axes are in pixels of 64 μm . The corresponding Reynolds number ($Re / (1 - \varepsilon)$) equals 51.

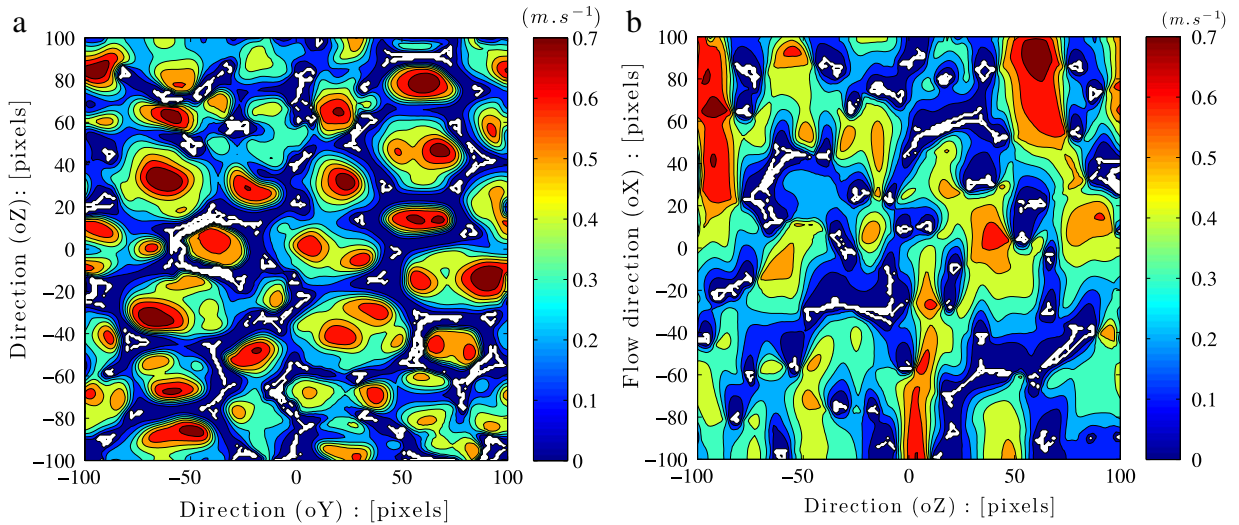


Fig. 2. Component of the velocity parallel to flow direction: (a) in a plane perpendicular to the flow direction and (b) in a plane parallel to the direction.

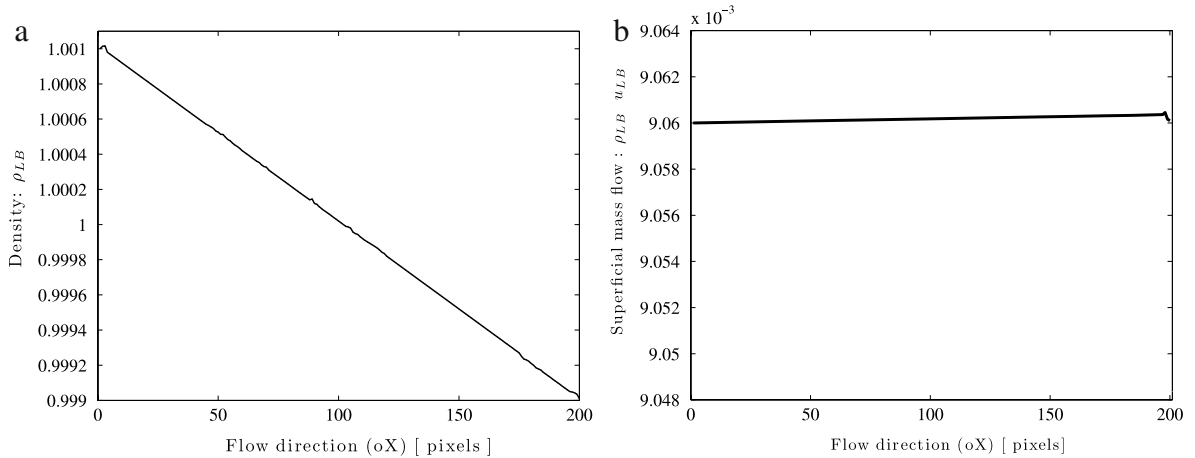


Fig. 3. (a) Pressure profile through the foam. (b) Momentum profile through the foam.

The no-slip boundary conditions “full way bounce back”, imposed to the solids is well observed: the macroscopic velocity is null on the walls. The white colour indicates the solid struts (Fig. 2). Fig. 3a and b represent pressure and momentum profiles through the foam. The pressure profile is linear in the flow direction and momentum is conserved. These results are in perfect agreement with the theory.

The pressure drop in the RCM-NCX-1116 metallic foam has been experimentally determined by [4].

Fig. 4 presents the evolution of pressure drop versus velocity (gas) and compares these data with simulated results at different sampling rates (e.g., a sampling rate of 2 means that one point on two from the initial sample is kept). The relative error between simulation and experimental data is lower or equal than 7%. The fitting of Eq. (15) on simulation data is given by:

$$\frac{\Delta P}{L} = \frac{\rho}{D_p} \frac{(1 - \varepsilon)}{\varepsilon^3} \left[77.85 \frac{(1 - \varepsilon)}{Re} + 0.77 \right] u^2. \quad (18)$$

Coefficients A and B in Eq. (18) allow estimating friction factor f_k using Eq. (12). These estimates illustrated in Fig. 5 confirm results presented in Fig. 4. We verify the relative error of 7% between simulation results and experimental data.

The agreement with the experimental data is quite good, in spite of the rusticity of the full way bounce back condition we used. However, it may be noticed that to obtain these results, we maintained the lattice Boltzmann viscosity constant to the value we got from Eq. (9) and we varied the pressure difference applied. This seemed to lead to more satisfactory results.

We observed that the flow simulated through the metallic foam is laminar. This result was observed also by [19–22]. Metallic foams are thus beds which present weak pressure drop.

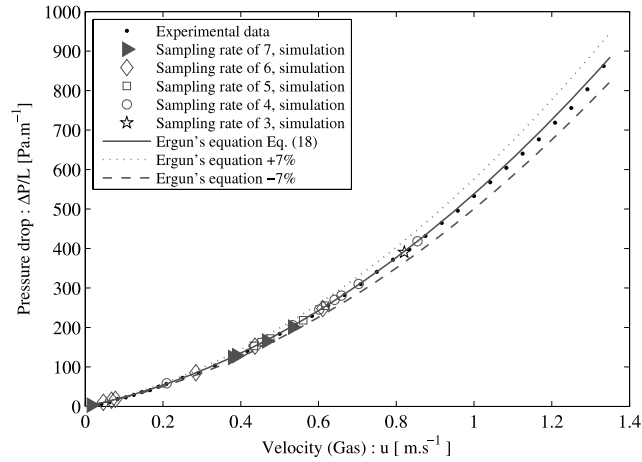


Fig. 4. Comparison between experimental and simulation data: correlation between $\Delta P/L$ and u .

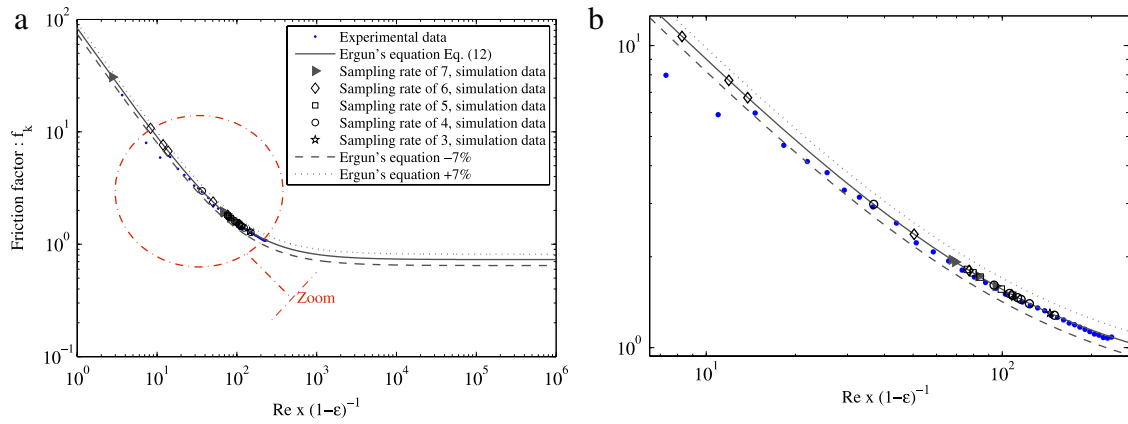


Fig. 5. The friction factor versus the Reynolds number: (a) Experimental data and simulation data and (b) zoom of the image in (a).

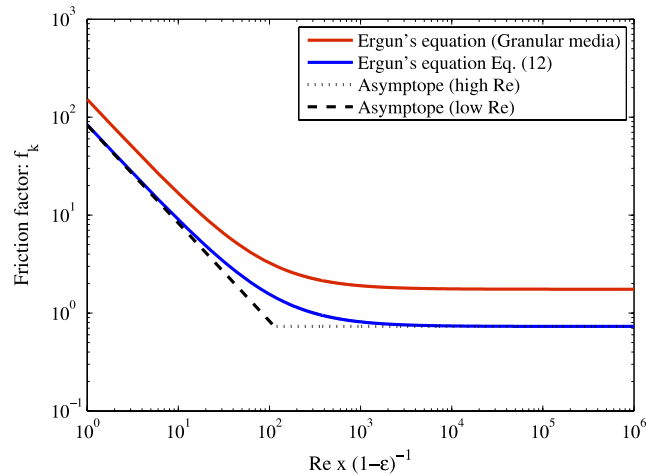


Fig. 6. Comparison of Ergun's equation fitted on simulation data Eq. (12) with Ergun's equation for granular media.

Fig. 6 classically illustrates the three regions of evolution of the friction factor versus the Reynolds number. In the low Reynolds region ($Re < 10$), the Darcy flow is observed with $f_k = (1 - \varepsilon) / Re$. For Reynolds numbers ranging between 10 and 2800, there is a transition zone, which can be described by $f_k = 77.85 (1 - \varepsilon) / Re + 0.77$ when Re is much larger than 2800, the quadratic term dominates and f_k approaches 0.77, the asymptotic value.

Table 1

Comparison of friction factors in granular media and metallic foam.

$Re/(1 - \varepsilon)$	1	120	1000	2800	∞
$f_{k,granular}$	151.75	3.00	1.90	1.81	1.75
$f_{k,foam}$	78.62	1.42	0.85	0.80	0.77
$f_{k,granular}/f_{k,foam}$	1.930	2.113	2.235	2.263	2.273

Fig. 6 allows also comparing pressure drop observed in the metallic foam with values classically reported for granular media (Ergun's equation with $A = 150$ and $B = 1.75$). Pressure drop in granular media was found to be one order magnitude higher than that observed and simulated in the metallic foam.

This confirms one of the advantages of the open cell structure of metallic foams, which results in a much more permeable material [23,24].

The ratio between friction factors in granular media and metallic foam is provided in Table 1 for different Reynolds number values. $f_{k,granular}/f_{k,foam}$ increased from 1.930 when $Re/(1 - \varepsilon) = 1$ to 2.263 when $Re/(1 - \varepsilon) = 2800$.

6. Conclusions and perspectives

Simulation results of pressure drop through metallic foam using lattice Boltzmann MRT codes are very promising. They confirm the ability of LB codes to compute the flow through intricate geometries resulting from computed X-ray micro-tomography. There is an encouraging agreement between simulations and the experimental results. Computation times are long but relatively inexpensive computing grids may be used with the developed LaBoGrid software [17].

The SRTLB–MRTLb code will be adapted in order to model two-phase flow through porous media by cellular automata.

Acknowledgment

This work was performed in the frame of the Research Concerted Action 05/10-334 supported by the Communauté Française de Belgique.

References

- [1] R. Caulkin, X. Jia, M. Fairweather, R.A. Williams, Lattice approaches to packed column simulations, *Journ of particuology* 6 (2008) 404–411.
- [2] A. Nabovati, E.W. Llewellyn, A.C.M. Sousa, A general model for the permeability of fibrous porous media based on fluid flow simulations using the lattice Boltzmann method, *Composites Part A: Appl. Sci. Manufactur.* 40 (2009) 860–869.
- [3] P. Marchot, D. Toye, M. Crine, A.-M. Pelsser, G. L'Homme, Investigation of liquid maldistribution in packed columns by x-ray tomography, *Trans. Inst. Chem. Eng* 77 (1999) 131–142.
- [4] S. Calvo, D. Beugre, M. Crine, A. Léonard, P. Marchot, D. Toye, Phase distribution measurements in metallic foam packing using x-ray radiography and micro-tomography, *Chem. Eng Process: Process Intensification* 48 (2009) 1030–1039.
- [5] F.J. Higuera, J. Jiménez, Boltzmann approach to lattice gas simulations, *Europhys. Lett* 9 (663) (1989).
- [6] G. McNamara, G. Zanetti, Use of the Boltzmann equation to simulate lattice-gas automata, *Phys. Rev. Lett* 61 (2332) (1988).
- [7] D. Yu, R. Mei, L.-S. Luo, W. Shyy, Viscous flow computations with the method of lattice Boltzmann equation, *Prog. Aerosp. Sci* 39 (329) (2003).
- [8] H. Chen, S. Chen, W.H. Matthaeus, Recovery of the Navier–Stokes equations using a lattice-gas Boltzmann method, *Phys. Rev. A* 45 (R5339) (1992).
- [9] P.L. Bhatnagar, E.P. Gross, M. Krook, A model for collision process in gases. I. Small amplitude process in charged and neutral one-component systems, *Phys. Rev* 94 (511) (1954).
- [10] X. He, L.-S. Luo, Lattice Boltzmann model for incompressible Navier–Stokes equation, *J. Comput. Phys* 88 (927) (1997).
- [11] E. Chapman, T.G. Cowling, *The Mathematical Theory of Non-Uniform Gases*, Cambridge University Press, 1970.
- [12] D. d'Humières, Generalized lattice Boltzmann equations, in: B.D. Shizgal, D.P. Weaver (Eds.), *Rarefied Gas Dynamics: Theory and Simulations*, vol. 159, AIAA, Washington, DC, 1992, pp. 450–458.
- [13] D. d'Humières, I. Ginzburg, M. Krafczyk, P. Lallemand, L.-S. Luo, Multiple-relaxation-time lattice Boltzmann models in three dimensions, *Proc. R. Soc. Lond. Ser., A* 360 (2002) 437.
- [14] H. Yu, L.-S. Luo, S.S. Girimaji, Les of turbulent square jet flow using an mrt lattice Boltzmann model, *Computers and Fluids* 35 (2006) 957–965.
- [15] F.A.L. Dullien, *Porous Media*, in: *Fluid Transport and Pore Structure*, Academy Press, INC, Waterloo, Ontario, Canada, 1979.
- [16] J. Comiti, et al., Experimental characterization of flow regimes in various porous media-iii: Limit of Darcy's or creeping flow regime for Newtonian and purely viscous non-Newtonian fluids, *Chem. Eng. Sci.* 55 (2000) 3057–3061.
- [17] G. Dethier, C. Briquet, P. Marchot, P.A. de Marneffe, A grid-enable lattice Boltzmann based modelling system, in: *Proc. International Conference on Parallel Processing and Applied Mathematics*, Gdansk, Poland, 2007.
- [18] I. Ginzburg, D. d'Humières, Multireflection boundary conditions for lattice Boltzmann models, *Phys. Rev. E* 68 (066614) (2003).
- [19] J. Comiti, M. Renaud, A new model for determining mean structure parameters of fixed beds from pressure drop measurements: Application to beds packed with parallelepipedal particles, *Chem. Engrg. Sci.* 44 (1989) 1539–1545.
- [20] D. Edouard, M. Lacroix, C.P. Huu, F. Luck, Pressure drop modeling on solid foam: State-of-the art correlation, *Chem. Eng. Sci.* 144 (2008) 299–311.
- [21] D. Seguin, A. Montillet, J. Comiti, Experimental characterisation of flow regimes in various porous media-i: Limit of laminar flow regime, *Chem. Engrg. Sci.* 53 (1998) 3751–3761.
- [22] G. Zhaoli, T.S. Zhao, Lattice Boltzmann model for incompressible flows through porous media, *Phys. Rev. E* 66 (036304) (2002).
- [23] C. Hongqing, Y. Hao, T. Yong, P. Mingqiang, P. Feng, W. Hongjuan, Y. Jian, Assessment and optimization of the mass-transfer limitation in a metal foam methanol microreformer, *Applied Catalysis A: General* 337 (2008) 155–162.
- [24] P.W.A.M. Wenmakers, J. Van der Schaaf, B.F.M. Kuster, J.C. Schouten, Hairy foam: Carbon nanofibers grown on solid carbon foam: A fully accessible, high surface area, graphitic catalyst support, *J. Mater. Chem.* 18 (2008) 2426–2436.